High-pressure phases in SnO_2 to 117 GPa

Sean R. Shieh*
Department of Earth Sciences, National Cheng Kung University, Taiwan 701

Atsushi Kubo and Thomas S. Duffy
Department of Geosciences, Princeton University, Princeton, New Jersey 08544, USA

Vitali B. Prakapenka and Guoyin Shen†
GeoSoilEnviroCARS, University of Chicago, Chicago, Illinos 60637, USA
(Received 25 August 2005; revised manuscript received 28 October 2005; published 13 January 2006)

X-ray diffraction of SnO_2 (cassiterite) at high pressures and temperatures demonstrates the existence of four phase transitions to 117 GPa. The observed sequence of phases for SnO_2 is rutile-type ($P4_2/mnm$) $\rightarrow$ $CaCl_2$-type($Pnnm$) $\rightarrow$ pyrite-type($Pa\bar{3}$) $\rightarrow$ ZrO_2 orthorhombic phase I ($Pbca$) $\rightarrow$ cotunnite-type ($Pnam$). Our observations of the first three phases are generally in agreement with earlier studies. The orthorhombic phase I and cotunnite-type structure (orthorhombic phase II) were observed in SnO_2 for the first time. The $Pbca$ phase is found at 50–74 GPa during room-temperature compression. The cotunnite-type structure was synthesized when SnO_2 was compressed to 74 GPa and heated at 1200 K. The cotunnite-type form was observed during compression between 54–117 GPa with additional laser heating carried out at 91 and 111 GPa. Fitting the pressure-volume data for the high-pressure phases to the second-order Birch-Murnaghan equation of state yields a bulk modulus of 259(26) GPa for the $Pbca$ phase and 417(7) GPa for the cotunnite-type phase.

DOI: 10.1103/PhysRevB.73.014105 PACS number(s): 62.50.+p, 61.10.Nz, 61.50.Ks, 64.10.+h

INTRODUCTION

There has been considerable interest in the high-pressure behavior of metal dioxides, MO_2, where M includes IVA and IVB cations such as Si, Ge, Sn, Pb, Ti, Zr, Hf. These materials exhibit extensive polymorphism at high pressures, and a variety of transformation pathways leading to highly coordinated structures have been uncovered.[1] Some high-pressure polymorphs in these systems have very high bulk moduli and hardness and may qualify as strong or even superhard solids.[2,3] The behavior of SiO_2 is of particular interest as this material is of widespread importance in geophysics and condensed matter physics. The other group-IVB dioxides (Ge, Sn, Pb) have been investigated as analogs for SiO_2, and they exhibit similar sequences of transitions but at lower pressures compared with silica. In all these materials, a sequence of phase transitions from rutile ($P4_2/mnm$) to $CaCl_2$-type ($Pnnm$) to α-PbO_2-type ($Pbcn$) to pyrite-type ($Pa\bar{3}$) have been found or predicted.[4–9]

The high-pressure behavior of cassiterite (SnO_2) has been the subject of many previous investigations extending up to 49 GPa.[5–7,10–15] In the earliest studies, transformation to the α-PbO_2-type structure and a cubic structure at higher pressures identified as fluorite-type were reported.[11,13,15] During room-temperature compression of SnO_2 to 49 GPa, Haines and Leger[5] first observed the rutile to $CaCl_2$-type transformation near 12 GPa. They also reported that the cubic phase was actually a modified-fluorite or pyrite-type structure instead of fluorite-type, not only in the case of SnO_2 but other metal dioxides as well.[4,5] Ono and colleagues[6,7] have carried out high P-T studies on SnO_2 using the diamond cell and large-volume press to ~30 GPa and 1500 K to investigate the transformations to the α-PbO_2-type and pyrite-type phases.

There are several lines of evidence to suggest that additional transitions at higher pressures are expected in this system. Investigation of PbO_2 shows a similar sequence of phase transitions as SnO_2, but the transformations occur at lower pressures, as expected due to the larger ionic radius of Pb.[4] In addition to the rutile-type, $CaCl_2$-type, α-PbO_2-type, and pyrite-type structures, a further transformation to an orthorhombic phase ($Pbca$; orthorhombic I) was found in PbO_2 at 11 GPa.[4] At 29 GPa, a cotunnite-type ($PbCl_2$) structure ($Pnam$, orthorhombic II) with nine-fold coordination was observed.[4] For group-IVA (Ti, Zr, Hf) metal dioxides, a different sequence of phases is observed at lower pressures, but both the orthorhombic I and cotunnite-type forms are found at higher pressures.[3,16–20] Theoretical calculations also indicate that the cotunnite form of SiO_2 may be stable at pressures of ~750 GPa.[8] In addition, shock compression data for cassiterite have also been reported.[21–23] There is evidence for one or more phase transitions, but the nature of the high-pressure phases is not known.

The high-pressure phases of metal dioxides have also attracted much attention because of their potential as superhard materials.[24] In particular, the dense, cotunnite-type form with nine-fold oxygen coordination is of great interest. It has been reported that cotunnite-structured TiO_2 is the hardest known oxide.[2] Bulk moduli in excess of 300 GPa have been determined from both theory and experiment on cotunnite-structured oxides such as TiO_2, HfO_2, and ZrO_2.[2,3,19,25,26]

EXPERIMENT

A natural sample was examined by x-ray diffraction and confirmed to be pure cassiterite (SnO_2). The lattice parameters for the rutile-structured starting material were a

$=4.746(1)$ Å and $c=3.189(1)$ Å. The powder sample was mixed with 10 wt. % platinum and loaded into a symmetric-type diamond anvil cell. A sample chamber was formed by drilling a $35-\mu$m diameter hole in a rhenium gasket that had been preindented to a thickness of ~ 20 μm. Platinum was used as a laser absorber and pressure standard. Pressure was determined from the equation of state of platinum.[27] Argon was used as a pressure-transmitting medium and for thermal insulation. Ruby chips were also loaded at the edge of the chamber, away from the sample to allow for pressure calibration during cryogenic argon loading.

In situ high-pressure synchrotron x-ray diffraction was carried out at the GeoSoilEnviroCARS (GSECARS) sector (13-ID-D) of the Advanced Photon Source.[28] A monochromatic beam with wavelength of 0.3344 Å was focused to $\sim 5\times 5$ μm^2 by a pair of 200-mm long Kirkpatrick-Baez mirrors. A MAR345 image plate detector was used to record two-dimensional images. CeO_2 powder was used to calibrate the distance and orientation of the detector. The two-dimensional x-ray diffraction images of SnO_2 were collected in the range of 30–60 seconds. The obtained diffraction images showed mostly smooth and uniform diffraction rings without major texture development. The program FIT2D[29] was used to reduce the two-dimensional images into one-dimensional patterns. Both peak fitting and the General Structure Analysis System (GSAS) program[30] were used for phase identification and data analysis. Le Bail profile fitting was initially carried out to obtain high-pressure cell constants. This whole-pattern fitting method involves adjusting the unit cell parameters and peak shape parameters to give the best fit to the observed data. Rietveld refinements were also carried out on selected patterns. A pseudovoigt profile function and spherical harmonic preferred orientation model were used. Initial atomic positions were taken from literature values. The background was manually subtracted before the refinement. The following parameters were refined: lattice parameters, peak shape parameters, phase fractions, atomic positions, averaged displacement parameters, and spherical-harmonic terms in preferred orientation correction.

High temperatures were achieved using double-sided heating[28,31] with the TEM_{00} mode of a Nd:YLF laser (1064-nm wavelength). Three heating cycles were conducted. The first heating was performed at 74 GPa with duration of 8 min. Two other heating cycles were conducted at 91 GPa and 111 GPa and with total heating time of 10 and 30 min, respectively. Based on visual observation of thermal radiation emitted from the sample, the heating was stable and uniform with a $20-30-\mu$m diameter at each pressure. The temperatures were measured by spectroradiometry and covered the range of 1200–2400 K. During the initial short heating, the temperatures were kept low and the laser beam was rastered across the entire sample. For the second heating cycle, the sample position was held fixed, and the higher laser power was required due to the higher pressure. For the third heating cycle, the sample was rastered again at still higher power.

RESULTS AND DISCUSSION

The pressure in the sample was gradually increased to 74 GPa at room temperature. During this compression, three

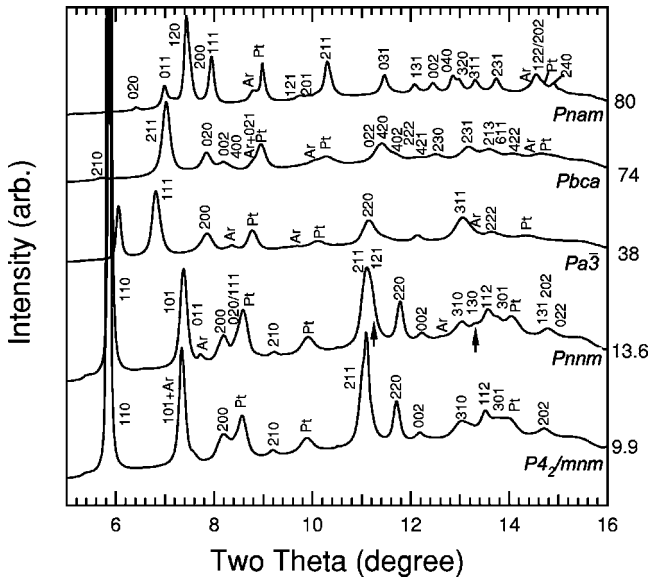

FIG. 1. Representative diffraction patterns for phases of SnO_2 observed in this study. Each trace is labeled with pressure (in GPa) and space group of corresponding structure. The abbreviations are Pt for platinum and Ar for argon. The arrows emphasize the splitting of peaks from $P4_2/mnm$ to *Pnnm*.

phase transitions were observed by x-ray diffraction. In a previous study,[5] SnO_2 in the rutile-type ($P4_2/mnm$) structure is observed to transform to orthorhombic $CaCl_2$-type structure (*Pnnm*) at 12.6 GPa under hydrostatic conditions. From Le Bail refinements, we identify the rutile phase at 9.9 GPa but could not exclude the possibility of the appearance of a minor amount of $CaCl_2$-type phase due to the broadening of the 211 peak. However, we did confirm the existence of the $CaCl_2$-type modification at 13.6 GPa (Fig. 1). The lattice parameters for the $CaCl_2$-type structure are $a=4.6781(7)$Å, $b=4.5361(8)$Å, $c=3.1443(5)$Å at 13.6 GPa. A previous study[5] reported that under nonhydrostatic conditions, the $CaCl_2$-type phase of SnO_2 was observed at pressure greater than 5 GPa and the α-PbO_2-type phase was found above 12.6 GPa. The same study showed that under hydrostatic conditions, the $CaCl_2$-type phase does not appear until pressures greater than 12 GPa. The unit cell parameters obtained in this work are compared to previous studies in Fig. 2. We observe a somewhat larger splitting between the *a* and *b* cell parameters of the $CaCl_2$-type (*Pnnm*) structure compared with the results of Ref. 5 under hydrostatic conditions (Methanol-ethanol-water medium). However, this splitting is smaller than that observed by nonhydrostatic decompression of the $CaCl_2$-type (*Pnnm*) phase using silicone grease as a pressure-transmitting medium.[5] This implies that the deviatoric stress state due to the solid Ar medium in this study is likely intermediate to those achieved in the hydrostatic and nonhydrostatic (silicone grease) experiments reported in Ref. 5. Peaks from the $CaCl_2$-type (*Pnnm*) structure were observed to persist up to 50 GPa during room-temperature compression. However, reliable lattice parameters of $CaCl_2$-type (*Pnnm*) structure can only be obtained at pressure to 28.8 GPa due to peak overlap with other high-pressure phases of SnO_2 and also due to the reduced peak intensities of *Pnnm* phase.

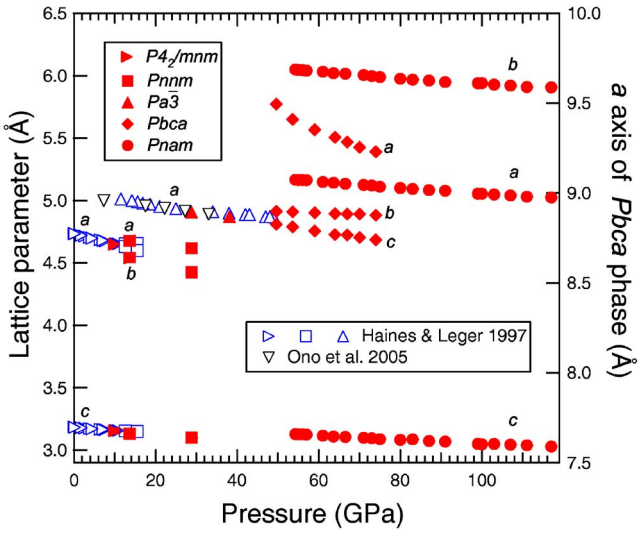

FIG. 2. (Color online) Variation of lattice parameters of SnO_2 phases as a function of pressure. The solid symbols are from this study; open symbols are from previous reports (Ref. 5,7). The $Pa\bar{3}$ data of Ref. 7 are shown with a down pointing triangle to distinguish them from the results of Ref. 5. Data obtained from $P4_2/mnm$, $Pnnm$, $Pa\bar{3}$, and $Pbca$ phases were without heating, whereas those of $Pnam$ phase were obtained after heating.

With further compression to 28.8 GPa, we observe changes to the diffraction pattern including a new peak near 6.8° (Fig. 1). Le Bail refinements indicate that this pattern consists of the low-pressure $Pnnm$ phase coexisting with the pyrite-type cubic structure ($Pa\bar{3}$). No α-PbO_2-type phase was observed in this study. This is not surprising as we overstepped most of its stability field, and the transformation is very sluggish during pressure increase without heating. In one study,[5] relatively small amounts of the α-PbO_2-type phase were observed under room-temperature compression of SnO_2 in the range of 12–21 GPa, while the sample recovered to ambient conditions from 49 GPa consisted of about half of this phase. In other studies, the α-PbO_2-type phase was observed at ~15–20 GPa after heating.[6,7,11,12] Similar observations[4] were reported during compression of plattnerite (rutile-structured PbO_2), which indicates the formation of the α-PbO_2-type phase requires thermal activation or high shear stresses.

The lattice parameter for the pyrite-type SnO_2 at 28.8 GPa obtained from Le Bail refinement is a=4.9052(3)Å. This is consistent with the result of Ono *et al.*[7] (a=4.9151 Å at 27.2 GPa) obtained after laser heating. After the next compression step to 38 GPa, our refinement result for the pyrite-type phase yields a=4.8728(4)Å which is in agreement with Haines and Leger[5] [a=4.8883(2)Å at 42 GPa]. Figure 2 compares the lattice constants obtained here with those of previous studies.[5,7] It should be noted that while no heating was applied at these pressures in this study, the results of the other studies were obtained after laser heating in some or all cases.

At 50 GPa, we observed that the 200, 220, and 311 peaks of the pyrite-type phase split indicating the existence of another phase. By analogy with the phase transition sequence

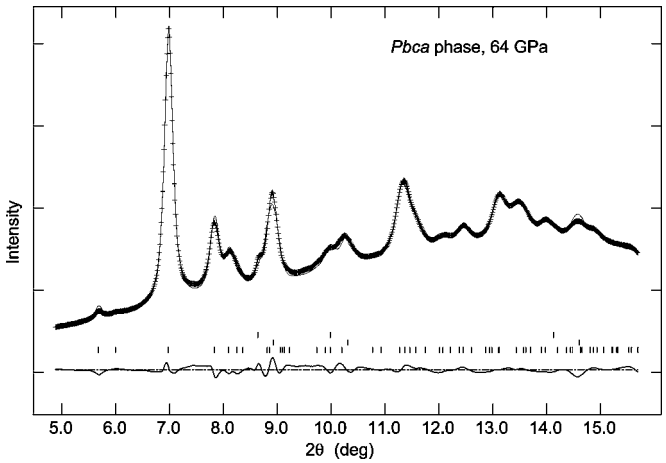

FIG. 3. Rietveld refinement result for $Pbca$ phase. The raw data (crosses) were obtained at 64 GPa, 300 K. The upper and lower solid curves are the calculated and difference curve ($I_{obs}-I_{calc}$), respectively. The short vertical bars above the difference curve show reflection positions for each phase (upper: Ar; middle: Pt; lower: $Pbca$ phase). The obtained lattice parameters are a=9.304(4) Å, b=4.8927(8) Å, c=4.731(2) Å, and atomic positions are Sn^{4+} [0.8906(4), 0.0254(6), 0.242(4)], O^{2-}(1): [0.810(5), 0.400(4), 0.143(8)], O^{2-}(2): [0.984(4), 0.738(20), 0.469(15)], and Rp=0.9%.

observed in PbO_2,[4] we found that this pattern could be described by the orthorhombic I phase ($Pbca$) of ZrO_2[4,32] (Fig. 3). We note that studies of ZrO_2, HfO_2, and PbO_2 have reported that several closely related structures could explain the diffraction pattern of this phase.[4,33] We were not able to distinguish among the different structures, and we have followed the assignment ($Pbca$) used previously. However, in fact, our Rietveld refinement for this phase using a$Pbca$ structural model yielded a very good fit (Rp=0.9%, Fig. 3 and Table I). The atomic positions obtained by this Rietveld refinement are very close to that of$Pbca$ phase in TiO_2 at 28 GPa by Rietveld refinement[17] and in PbO_2 at 26 GPa by partial Rietveld refinement.[4] In this$Pbca$ structural model, seven oxygen anions are placed around a Sn^{4+} cation at distances in the range 1.85 to 2.14Å. The mean Sn-O distance at 64 GPa is 2.015Å. The transition of $Pa\bar{3}$ to $Pbca$ structure can be clearly identified by the peak splittings observed at two theta near 8°, 11°, and 13° (Fig. 1). With increasing pressure, the peak splittings continued to grow. The $Pbca$ phase was found to be stable to 74 GPa at room temperature (Fig. 1). The evolution of lattice parameters for this phase is plotted in Fig. 2.

In the $Pbca$ phase, the orthorhombic cell exhibits a near doubling of the cell axis along a relative to the $Pa\bar{3}$ phase (Fig. 2). Fitting the b and c axes to linear functions and extrapolating to lower pressures indicate that the b and c axes would overlap at pressure near 22 GPa. In addition, the linear compressibilities of the $Pbca$ phase are in the sequence of $\beta_a > \beta_c > \beta_b$. As found in the case of PbO_2,[4] the compression of the $Pbca$ phase is highly anisotropic. In fact, we find that the b axis decreases by only ~0.5% from 50 to 74 GPa, compared with a decrease of ~3.5% and 2.6% for the a and c axes, respectively, over this pressure range. The volume change from $Pa\bar{3}$ to $Pbca$ is about 3% (Fig. 4). The

TABLE I. Results of Rietveld refinement of orthorhombic phase I (*Pbca*) of SnO_2 at 64 GPa and 300 K. Unit cell parameters obtained by Rietveld refinement are a=9.3039(35) Å, b=4.8927(8) Å, c=4.7315(16) Å.

hkl	*d*(Å)	I_{cal}
200	4.6520	4
210	3.3713	3
211	2.7456	100
020	2.4463	29
002	2.3658	12
400	2.3260	6
021	2.1731	3
221	1.9689	2
212	1.9365	2
411	1.9200	8
022	1.7006	20
420	1.6771	14
402	1.6586	9
222	1.5972	2
421	1.5879	2
230	1.5391	5
231	1.4636	19
213	1.4286	12
611	1.4109	7
422	1.3728	7

bulk modulus of the *Pbca* structure determined from fitting to a second-order Birch-Murnaghan equation of state yields 259(26) GPa and a zero-pressure volume of 256.4(34)Å^3 (Table II). This bulk modulus is lower than some previous determinations of the bulk modulus for the pyrite-type phase in SnO_2 (Table II). An anomalous decrease in the bulk modulus across this high-pressure phase transition was also reported for PbO_2.[4] Bulk moduli for the *Pbca* phase in the range of 210–318 GPa have been reported for HfO_2 and TiO_2.[3,17,34]

At 74 GPa, the sample was heated at 1200–1500 K for 8 min while being rastered. Upon quenching, the diffraction pattern was found to be different and the sample pressure dropped considerably to 54 GPa. Again, by comparison with the behavior of the PbO_2 system,[4] we are able to fit this pattern to a cotunnite-type structure (*Pnam*) (Fig. 5). The cotunnite-type phase was found to be stable upon further compression to 117 GPa and 2400 K (Table III) including two more heating cycles (at 91–99 GPa and 111–117 GPa). The experiment ended abruptly when a diamond shattered during heating at the highest pressure. It should be noted that the most intense peak of the orthorhombic phase I (211) was still observable (but weak) in the quenched diffraction pattern after the heating cycle at 54–74 GPa. This residual peak disappeared when the pressure was increased above 80 GPa (Fig. 1). Our Rietveld refinement for the *Pnam* phase yielded a good fit (Rp=1.2%) with atomic positions in good agreement with other cotunnite-type structures.[26] In the *Pnam* structure, nine oxygen anions are placed around a Sn^{4+} cation

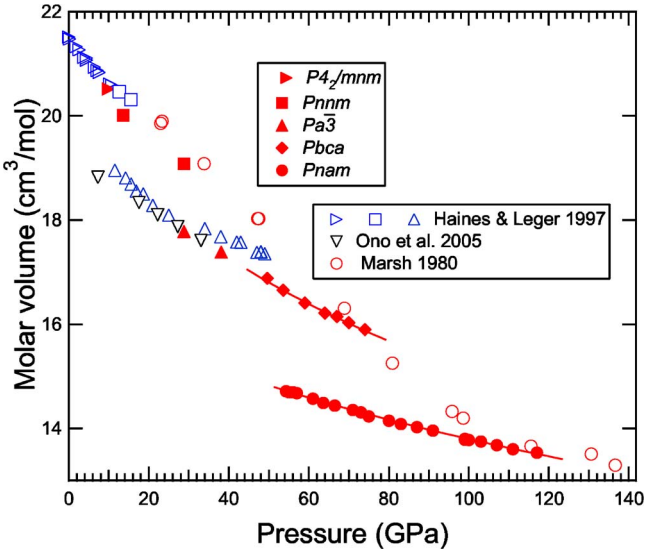

FIG. 4. (Color online) The molar volume as a function of pressure for SnO_2 phases at pressure to 117 GPa. The symbols used here are same as Fig. 2, except for open circles which represent shock compression data from Marsh (Ref. 22). Solid lines are second-order Birch-Murnaghan equation fits to *Pbca* and *Pnam* phase data. The $Pa\bar{3}$ data of Ref. 7 are shown with a down pointing triangle to distinguish them from the results of Ref. 5.

and we find distances ranging from 1.70 to 2.26 Å (at 117 GPa). The mean Sn-O distance at 117 GPa is 2.06 Å. The increase of mean Sn-O distance compared to that of *Pbca* phase is consistent with an increase of coordination number of tin ions from seven to nine by the transition of *Pbca* to *Pnam* phase.

The variation of the lattice parameters of cotunnite-type structure of SnO_2 upon compression is plotted in Fig. 2. The axial compressibilities for this phase at 55 GPa were found to be 5.4×10^{-4} GPa^{-1}, 4.5×10^{-4} GPa^{-1}, and 6.2×10^{-4} GPa^{-1} for the a, b, and c axes, respectively. Thus, the phase exhibits only modest anisotropy in compression behavior. As the pressure increases, the anisotropy of the compressibility is reduced somewhat further and the corresponding compressibilities at 115 GPa become 4.0×10^{-4} GPa^{-1}, 3.5×10^{-4} GPa^{-1}, and 4.4×10^{-4} GPa^{-1}. The volume change from *Pbca* to *Pnam* is about 11%, larger than that of the $Pa\bar{3}$ phase to *Pbca* phase. The reported volume change for the *Pbca-Pnam* transition in PbO_2 was 7.5%.[4] The bulk modulus of cotunnite-type structure determined from fitting the data to a second-order Birch-Murnaghan equation of state is 417(7) GPa and the obtained zero-pressure volume is 108.7(2) Å^3 [or 16.37(3) cm^3/mol] (Fig. 4, Table II).

The large bulk modulus of the cotunnite-type phase is comparable with those reported for the same structure type in ZrO_2[K_0=444(15) GPa][3] and TiO_2[K_0=431(10) GPa][2] but somewhat higher than in HfO_2[K_0=340(10) GPa].[3] The very high bulk modulus suggests cotunnite-type SnO_2 could be a strong or even superhard material. However, some caution is needed in interpreting these findings. The minimum pressure at which the cotunnite-type phase was observed was 54 GPa, and thus, there is significant extrapolation involved in deter-

TABLE II. Comparison of zero-pressure volume (V_0) and bulk modulus (K_0) of SnO_2 polymorphs. DAC—x-ray diffraction in diamond anvil cell; multianvil—x-ray diffraction in multianvil apparatus; ultrasonic—ultrasonic measurement of acoustic wave velocity; K_0'—pressure derivative of the bulk modulus.

Phase	V_0(Å^3)	K_0(GPa)	K_0'	Remark
$P4_2/mnm$	71.326	205(7)	7.4(2.0)	DAC[a]
		203		Ultrasonic[b]
		212	5.5	Ultrasonic[c]
		181		Theory[d]
Pnnm		204(6)	8(1)	DAC[a]
Pbcn	141.03	208(2)	4	DAC[a]
		199(4)	4	DAC[e]
$Pa\bar{3}$	128.1(3)	307(10)	4	DAC[f]
	129.4(4)	328(16)	4	DAC[a]
	130.6(3)	246(9)	4	Multianvil[f]
Pbca	256.4(34)	259(26)	4	This study
Pnam	108.7(2)	417(7)	4	This study

[a]See Ref. 5.
[b]See Ref. 36.
[c]See Ref. 37.
[d]See Ref. 38
[e]See Ref. 39
[f]See Ref. 7

mining the bulk modulus at ambient pressure. Also, the sample was only heated at three compression steps. Deviatoric stresses, which tend to lead to overestimation of the bulk modulus, may not be negligible. In fact, evidence for existence of deviatoric stress in Pt was observed during the Rietveld refinements. Theoretical studies[24] for cotunnite-type ZrO_2, TiO_2, and HfO_2 using density functional theory yield bulk moduli of ~300 GPa, which are considerably lower than diamond cell results.[2,3] Also, compression experiments[34] on HfO_2 and ZrO_2 using the multianvil press and energy-dispersive diffraction have also yielded lower

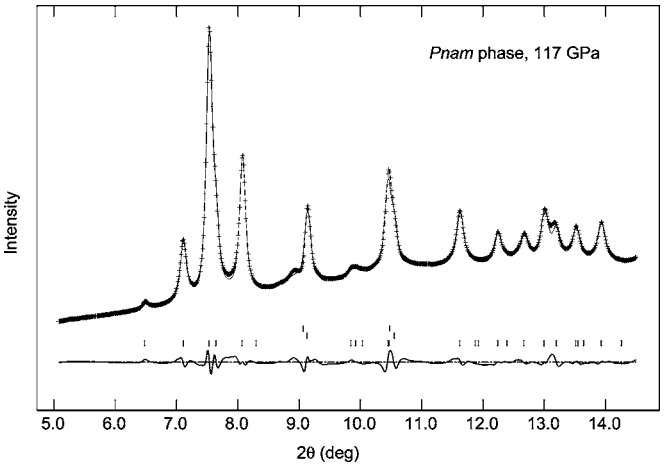

FIG. 5. Rietveld refinement result for *Pnam* phase. The raw data (crosses) were obtained at 117 GPa, 300 K (after heating). The upper and lower solid lines represent the calculated and the difference curves ($I_{obs}-I_{calc}$), respectively. The short vertical bars above the difference curve show reflection positions for each phase (upper: Ar; middle: Pt; lower: *Pnam* phase). The obtained atomic positions are Sn^{4+} [0.2547(18), 0.11422(31), 0.25], O^{2-}(1): [0.348(4), 0.390(5), 0.25], O^{2-}(2): [0.043(6), 0.333(4), 0.75], and Rp=1.2 %.

TABLE III. Results of Rietveld refinement of cotunnite-type structure (*Pnam*) of SnO_2 at 117 GPa and 300 K. Unit cell parameters obtained by Rietveld refinement are a=5.0156(6) Å, b=5.9044(3) Å, c=3.0282(3) Å.

hkl	d(Å)	I_{cal}
020	2.9522	2
011	2.6945	23
120	2.5442	100
200	2.5078	24
111	2.3736	54
121	1.9479	1
201	1.9315	2
211	1.8321	33
031	1.6502	21
131	1.5676	10
002	1.5141	10
040	1.4761	20
320	1.4548	12
311	1.4206	11
231	1.3785	15
122	1.3011	8
202	1.2962	7
240	1.2721	9
400	1.2539	2

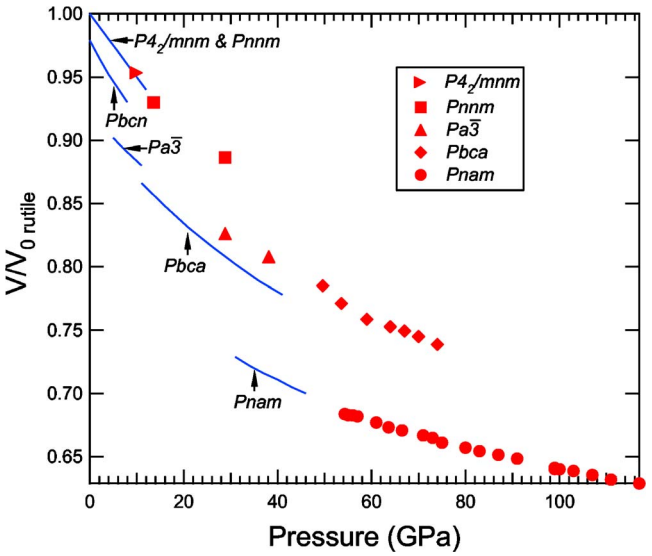

FIG. 6. (Color online) Comparison of compression behavior of PbO_2 (solid lines) with SnO_2 (symbols). For each phase, the volume is plotted relative to the zero-pressure volume of the rutile form for that material. Data for PbO_2 are from Ref. 4, data for SnO_2 are from this study.

bulk moduli for these materials, although these were obtained using a lower resolution diffraction technique. Very recent diamond anvil cell results on the cotunnite form of ZrO_2 yielded $K_0=278$ GPa.[20] The bulk modulus of the cotunnite-type phase of PbO_2 was reported to be 221 GPa.[4] Further exploration of bulk modulus systematics for the cotunnite-structured form of the group-IVA and, group-IVB elements is needed to resolve these discrepancies.

The overall similarity in compression behavior of SnO_2 and PbO_2 is illustrated in Fig. 6, which shows the compression data obtained here for SnO_2 compared to trends from previous data[4] for PbO_2. Measured volumes for both phases are plotted relative to the V_0 value of the corresponding rutile-type phase at ambient P and T. The relative volumes for the SnO_2 phases generally overlap or follow the extension of the lower pressure trend defined by the PbO_2, although the *Pbca* form appears to be somewhat less compressible for SnO_2.

While our overall results are generally consistent with those observed for PbO_2, there are some differences. In the case of PbO_2, the transformation from the orthorhombic I to cotunnite-type structure at 29 GPa was observed at room temperatures (without any heating) under relatively nonhydrostatic conditions (silicone grease as pressure medium).[4] The transition was also very sluggish and a mixture of low-pressure and high-pressure phases coexisted to 47 GPa. In contrast, we did not observe any transformation from the orthorhombic I phase up to 74 GPa at room temperature, but found almost complete and rapid transformation to the new structure after a short period of laser heating. In the case of ZrO_2, room-temperature transformation was observed at 16 GPa,[35] whereas the transformation occurred at ~10 GPa for a sample heated to 1000 °C,[12] indicating that the transformation pressure is significantly lower in the case of heating, which is consistent with our findings.

Figure 4 compares the static pressure-volume curve to shock compression data for cassiterite.[22] The shock data show evidence for two discontinuities along the Hugoniot curve, one above 47 GPa and another reaching completion around 115 GPa. Because thermal effects on the shock compression curve have not been accounted for, only qualitative conclusions can be drawn here. However, comparison of the two data sets suggests possible interpretation of the shock data. Under shock loading, the low-pressure form appears to remain stable to ~50 GPa, whereupon it transforms with a volume change consistent with that observed for the formation of the orthorhombic phase I which is the stable form at 300 K at these pressures. Finally, at higher shock pressures beginning around 80 GPa and extending to 115 GPa, cassiterite gradually adopts a denser form that is also consistent with the volume change observed here between the *Pbca* and cotunnite-type forms. Thus, we propose that the two high-pressure phases observed during shock compression of SnO_2 may be the orthorhombic phase I and cotunnite-type forms. At lower pressures, shock temperatures may be too low to drive the transformations leading up to the pyrite-type phase.

In summary, a sequence of four phase transitions is observed during compression and heating of SnO_2 to 117 GPa. The sequence of phases is consistent with previous observations for PbO_2.[4] The ZrO_2-type (*Pbca*) and cotunnite-type (*Pnam*) phases at pressure greater than 50 GPa are reported for the first time in SnO_2. The bulk modulus for the *Pbca* and *Pnam* phase of SnO_2 determined fitting pressure-volume data to the second-order Birch-Murnaghan equation of state are 259(26) and 417(7) GPa, respectively.

ACKNOWLEDGMENTS

The research was supported by NSF and C-DAC (DOE). Experiments were performed at GeoSoilEnviroCARS (Sector 13), Advanced Photon Source (APS), Argonne National Laboratory. GeoSoilEnviroCARS is supported by the National Science Foundation—Earth Sciences (Contract No. EAR-0217473), Department of Energy—Geosciences (Contract No. DE-FG02-94ER14466), and the state of Illinois. Use of the APS was supported by the U.S. Department of Energy, Basic Energy Sciences, Office of Science, under Contract No. W-31-109-Eng-38.

*Present address: Department of Earth Sciences, University of Western Ontario, Ontario, N6A 5B7.
†Present address: HPCAT, Advanced Photon Source, ANL, Argonne, IL 60439.

[1] J. M. Leger, J. Haines, Eur. J. Solid State Inorg. Chem. **34**, 785 (1997).
[2] L. S. Dubrovinsky, N. A. Dubrovinskaia, V. Swamy, J. Muscat, N. M. Harrison, R. Ahuja, B. Holm, and B. Johansson, Nature (London) **410**, 653 (2001).
[3] S. Desgreniers and K. Lagarec, Phys. Rev. B **59**, 8467 (1999).
[4] J. Haines, J. M. Leger, and O. Schulte, J. Phys.: Condens. Matter **8**, 1631 (1996).
[5] J. Haines and J. M. Leger, Phys. Rev. B **55**, 11144 (1997).
[6] S. Ono, E. Ito, T. Katsura, A. Yoneda, M. J. Walter, S. Urakawa, W. Utsumi, and K. Funakoshi, Phys. Chem. Miner. **27**, 618 (2000).
[7] S. Ono, K. Funakoshi, A. Nozawa, and T. Kikegawa, J. Appl. Phys. **97**, 073523 (2005).
[8] A. R. Oganov, M. J. Gillan, and G. D. Price, Phys. Rev. B **71**, 064104 (2005).
[9] Y. Kuwayama, K. Hirose, N. Sata, and Y. Ohishi, Science **309**, 923 (2005).
[10] R. L. Clendenen and H. G. Drickamer, J. Chem. Phys. **44**, 4223 (1965).
[11] L. Liu, Phys. Earth Planet. Inter. **9**, 338 (1974).
[12] K. Suito, N. Kawai, and Y. Masuda, Mater. Res. Bull. **10**, 677 (1975).
[13] L. Liu, Science **199**, 422 (1978).
[14] L. C. Ming and M. H. Manghnani, in *High-Pressure Research in Geophysics*, edited by S. Akimoto and M. H. Manghnani (Center for Academic Publication, Tokyo, 1982), p. 329.
[15] S. Endo, S. Nitawaki, T. Shige, Y. Akahama, T. Kikegawa, and O. Shimomura, High Press. Res. **4**, 408 (1990).
[16] J. Haines, J. M. Leger, and A. Atouf, J. Am. Ceram. Soc. **80**, 1910 (1997).
[17] N. A. Dubrovinskaia, L. S. Dubrovinsky, R. Ahuja, V. B. Prokopenko, V. Dmitriev, H. P. Weber, J. M. Osorio-Guillen, and B. Johansson, Phys. Rev. Lett. **87**, 275501 (2001).
[18] O. Ohtaka, H. Fukui, T. Kunisada, T. Fujisawa, K. Funakoshi, W. Utsumi, T. Irifune, K. Kuroda, and T. Kikegawa, Phys. Rev. B **63**, 174108 (2001).
[19] R. Ahuja and L. S. Dubrovinsky, J. Phys.: Condens. Matter **14**, 10995 (2002).
[20] O. Ohtaka, D. Andrault, P. Bouvier, E. Schultz, and M. Mezouar, J. Appl. Crystallogr. **38**, 727 (2005).
[21] G. V. Simakov, M. A. Podurets, and R. F. Trunin, Dokl. Akad. Nauk SSSR **211**, 1330 (1973).
[22] S. P. Marsh, *LASL Shock Hugoniot Data* (University of California Press, Los Angeles, CA, 1980) p. 658.
[23] T. J. Ahrens and M. L. Johnson, in *Mineral Physics and Crystallography*, edited by T. J. Ahrens (American Geophysical Union, Washington DC, 1995), p. 143.
[24] J. E. Lowther, Phys. Status Solidi B **217**, 533 (2000).
[25] J. Haines, J. M. Leger, and A. Atouf, J. Am. Ceram. Soc. **78**, 445 (1995).
[26] J. K. Dewhurst and J. E. Lowther, Phys. Rev. B **64**, 014104 (2001).
[27] N. C. Holmes, J. A. Moriarty, G. R. Gathers, and W. J. Nellis, J. Appl. Phys. **66**, 2962 (1989).
[28] G. Shen, V. B. Prakapenka, P. J. Eng, M. L. Rivers, S. R. Sutton, J. Synchrotron Radiat. **12**, 642 2005.
[29] A. P. Hammersley, S. O. Svensson, M. Hanfland, A. N. Fitch, and D. Hausermann, High Press. Res. **14**, 235 (1996).
[30] A. C. Larson and R. B. Von Dreele, Los Alamos National Lab. Report No. LA-UR-86-748, 1987 (unpublished).
[31] G. Shen, M. L. Rivers, Y. Wang, and S. R. Sutton, Rev. Sci. Instrum. **72**, 1273 (2001).
[32] O. Ohtaka, T. Yamanaka, S. Kume, N. Hara, H. Asano, and F. Izumi, Proc. Jpn. Acad., Ser. B: Phys. Biol. Sci. **66**, 193 (1990).
[33] J. E. Lowther, J. K. Dewhurst, J. M. Leger, and J. Haines, Phys. Rev. B **60**, 14 485 (1999).
[34] O. Ohtaka, H. Fukui, K. Funakoshi, W. Utsumi, T. Irifune, and T. Kikegawa, High Press. Res. **22**, 221 (2002).
[35] S. Block, J. A. H. da Jornada and G. J. Piermarini, J. Am. Ceram. Soc. **68**, 497 (1985).
[36] R. C. Liebermann, Phys. Earth Planet. Inter. **7**, 461 (1973).
[37] E. Chang and E. K. Graham, J. Geophys. Res. **80**, 2595 (1975).
[38] E. L. Peltzer y Blanca, A. Svane, N. E. Christensen, C. O. Rodriguez, O. M. Cappannini, and M. S. Moreno, Phys. Rev. B **48**, 15712 (1993).
[39] S. Endo, S., Nitawaki, T. Shige, Y. Akahama, T. Kikegawa, and O. Shimomura, High Press. Res. **4**, 408 (1990).